

YerPhI Preprint 1623 (2010)

**NUCLEAR EFFECTS IN REACTIONS $\nu p \rightarrow \mu^- p \pi^+$ and
 $\nu p \rightarrow \mu^- \Delta^{++}(1232)$ ON BOUND PROTONS**

SKAT Collaboration

N.M. Agababyan¹, N. Grigoryan², H. Gulkanyan², A.A. Ivanilov³,
Zh. Karamyan², V.A. Korotkov³

¹ Joint Institute for Nuclear Research, Dubna, Russia

² Yerevan Physics Institute, Armenia

³ Institute for High Energy Physics, Protvino, Russia

YEREVAN 2010

Abstract

For the first time, the nuclear effects in the reaction $\nu p \rightarrow \mu^- p \pi^+$ on bound protons are investigated at $\langle E_\nu \rangle \approx 9$ GeV and the effective atomic weight $A_{\text{eff}} \approx 21$ of the composite nuclear target using the data obtained with SKAT bubble chamber. The observed nuclear effects are explained by the Fermi-motion of the target proton and secondary elastic scattering of neutrino-produced hadrons on intranuclear neutrons. The probability of any intranuclear interaction of neutrino-produced hadrons is extracted: $P_{\text{int}} = 0.40 \pm 0.13$, while the probability of interactions occurring only via elastic scattering on intranuclear neutrons is estimated to be $P_c = 0.14 \pm 0.05$.

A clear evidence of the $\Delta^{++}(1232)$ and an indication on the $\Delta^{++}(1620)$ isobar states production are observed with the mean yields, respectively, 0.57 ± 0.09 and 0.40 ± 0.26 (the latter being corrected for the $p\pi^+$ decay fraction). The mean yield of $\Delta^{++}(1232)$ is by 1.61 ± 0.25 times smaller than expected for the reaction on the hydrogen target, thus indicating on its rather strong nuclear absorption.

1. INTRODUCTION

In the space-time pattern of the leptonproduction on nuclear targets an important role belongs to hadron resonances which cause a significant fraction of final hadrons (see [1] and references therein). A fraction of short-living resonances (like ρ, Δ etc.) decays inside the nucleus followed by secondary intranuclear interactions of the decay products, resulting in a deterioration of their effective mass distribution (i.e. the resonance spectral function). Moreover, the latter can be distorted also at the propagation of resonances inside the nuclear medium due to their interactions with intranuclear nucleons (for example, via the channel $\Delta N \rightarrow NN$) reducing their lifetime, i.e. widening their spectral function. The Pauli blocking for the decay of barionic resonances, on the contrary, leads to the increasing of the resonances lifetime, i.e. to the decreasing of their width. The nuclear effects can also induce a mass shift of resonances (see [2, 3, 4] and references therein).

Lepton-induced exclusive reactions on intranuclear nucleons are convenient processes to observe the nuclear effects in the resonance production. The aim of this work is the investigation of nuclear effects in neutrino-induced single-pion production reaction on intranuclear protons

$$\nu + p \rightarrow \mu^- + p + \pi^+, \quad (1)$$

which includes both the $\Delta^{++}(1232)$ production,

$$\nu + p \rightarrow \mu^- + \Delta^{++}(1232), \quad (2)$$

and the nonresonant π^+ production.

To this end, the data from the SKAT bubble chamber [5] were used. In Section 2 the experimental procedure is described. Section 3 presents the observed kinematic characteristics of the reaction (1) and their description in terms of nuclear effects. Section 4 is devoted to the study of the reaction (2), with a particular emphasis on the nuclear effects influence on the yield of $\Delta^{++}(1232)$. The results are summarized in Section 4.

2. EXPERIMENTAL PROCEDURE

The experiment was performed with SKAT bubble chamber, exposed to a wideband neutrino beam obtained with a 70 GeV primary protons from the Serpukhov accelerator. The chamber was filled with a propane-freon mixture containing 87 vol% propane (C_3H_8) and 13 vol% freon (CF_3Br) with the percentage of nuclei H:C:F:Br = 67.9:26.8:4.0:1.3 % and the effective atomic weight $A_{\text{eff}} \approx 21$ of the composite (C, F, Br) nuclear target. A 20 kG uniform magnetic field was provided within the operating chamber volume.

Charged (CC) current interactions containing a negative muon with momentum $p_\mu > 0.5$ GeV/c were selected. Protons with momentum below 0.6 GeV/c and a fraction of protons with momentum 0.6-0.85 GeV/c were identified by their stopping in the chamber. Stopping π^+ mesons were identified by their $\pi^+ \rightarrow \mu^+ e^+$ decay. A fraction of low-momentum ($p_{\pi^+} < 0.5$ GeV/c) π^+ mesons were identified by the mass-dependent fit provided that the χ^2 -value for the pion hypothesis was significantly smaller as compared to that for proton. It was required the errors in measuring the momenta be less than 24% for muon, 60% for other charged particles and V^0 's (corresponding to strange particles) and less than 100% for photons. Each event was given a weight to correct for the fraction of events excluded due to improperly reconstruction. More details concerning the experimental procedure,

in particular, the reconstruction of the neutrino energy E_ν , can be found in our previous publications [6, 7].

Events with $3 < E_\nu < 30$ GeV were selected, provided that the summary momentum of produced hadrons is directed forward respective to the neutrino direction, resulting in 8237 events (or $N_{\text{tot}} = 9631$ weighted events) with the mean neutrino energy $\langle E_\nu \rangle = 9.1$ GeV. The contamination from the neutral current (NC) interactions was estimated to be about 4%.

We chosen the events-candidates to the reaction (1) containing two positively charged hadrons and no registered γ -quanta or V^0 - particles. In the most fraction (69%) of the chosen events, at least one of the hadrons was identified as π^+ - meson or proton. The remaining 31% of events (with two non-identified hadrons) were weighted by an additional factor of 0.5, because they entered twice in the distributions discussed in the next sections. The proton (identified or being a unidentified candidate to proton) is required to be emitted in the forward direction in the laboratory frame and to have a momentum $P_p > 0.2$ GeV/ c in order to reduce the contamination from the nuclear disintegration products. The problems related with the background events with misidentified positively charged hadrons are discussed below in this and next sections.

Further, we rejected events for which the energy momentum disbalances p_L^{miss} and p_T^{miss} (defined analogously to those in the next section) were compatible with the kinematics of the quasielastic reaction $\nu n \rightarrow \mu^- p$ followed by a secondary elastic pp scattering with at least one non-identified proton in the final state. The rejected events was satisfying the requirements $|p_L^{\text{miss}}| < 0.1$ GeV/ c and $p_T^{\text{miss}} < 0.25$ GeV/ c , the quoted boundaries being chosen so that the number of rejected events (19 events) was equal to that estimated from the differential cross section of the reaction $\nu n \rightarrow \mu^- p$ and the probability of a secondary pp scattering resulting in at least one non-identified proton in the final state.

We also excluded the events containing a registered neutron and being compatible with the kinematics of the reaction $\nu p \rightarrow \mu^- \pi^+ \pi^+ n$, namely, when the angle φ_n between the neutron direction and the direction of the summary momentum of the $\mu^- \pi^+ \pi^+$ system in the transverse plane (perpendicular to the neutrino direction) exceeded 143° (i.e. $\cos \varphi_n < -0.8$). We kept other events containing registered neutrons a part of which can originate from secondary elastic scattering of neutrino-produced hadrons on intranuclear neutrons – a process which is one of the subjects of the present study.

The total number of accepted events-candidates to the reaction (1), composing a subsample B_1 , was equal to 802. The contamination from the NC events is found to be equal to $2.2 \pm 0.5\%$. The contamination from the background CC events which could contain non-registered neutral particles was estimated to be $9 \pm 1\%$, using events with registered neutral particles weighted by a probability that a given event could potentially pass the aforementioned selection criteria.

It should be also stressed that a fraction of the subsample B_1 corresponds to the exclusive reaction (1) on the hydrogen. The number N_p^{free} of these events, estimated from the total number of events N_{tot} , the total cross section of νp and νn CC interactions [8, 9] and the cross section of the reaction (1) on free protons [8, 10, 11] at $\langle E_\nu \rangle = 9.1$ GeV, is equal to $N_p^{\text{free}} = 115 \pm 21$. Similarly, the expected event number of the reaction (1) occurring on bound protons (both followed or not by any intranuclear secondary interaction) is estimated to be $N_p^{\text{bound}} = 411 \pm 65$. The sum of $N_p^{\text{free}} + N_p^{\text{bound}}$ turns out to be smaller than the number of events in the subsample B_1 , contrary to what was expected due to the loss of events caused by secondary inelastic interactions of neutrino-produced proton, π^+ meson or Δ^{++} . We conclude, therefore, that the subsample B_1 contains a significant fraction of background

events corresponding to a number competing processes (considered in details in the next section).

3. THE CHARACTERISTICS OF THE REACTION (1) ON INTRANUCLEAR PROTONS

As compared to the reaction on the hydrogen target, the kinematic characteristics of the reaction (1) on intranuclear protons suffer distortions reflecting the effects of the Fermi-motion of the bound proton and the secondary intranuclear scattering of neutrino-produced hadrons. These result in an apparent violation of the energy-momentum balance of the reaction. Another source of distortions are experimental uncertainties inherent for both hydrogen and nuclear events. The energy-momentum unbalance can be characterized by 'missing' longitudinal (p_L^{miss}) and transverse (p_T^{miss}) momenta defined as

$$p_L^{miss} = \sum_i (E^i - p_L^i) - m \quad (3)$$

$$(p_T^{miss})^2 = \left(\sum_i \vec{p}_T^i \right)^2, \quad (4)$$

where the sums are over energies E^i , longitudinal p_L^i and transverse \vec{p}_T^i momenta (with respect to the neutrino direction) of final particles; m is the proton mass.

Figure 1 shows the distributions on p_L^{miss} and p_T^{miss} for the B_1 subsample, from which the corresponding distributions for the background events (see Section 2 above) were subtracted. As it will be shown below, the characteristic peaks at low values of $|p_L^{miss}|$ and p_T^{miss} reflect mainly the interactions on the hydrogen and, partly, on bound protons, when final hadrons escape secondary intranuclear interactions.

In general, the following process can contribute to the plotted distributions: *a)* the reaction (1) on hydrogen; *b)* the reaction (1) on bound protons not followed by any secondary interaction; *c)* the reaction (1) on bound protons followed by elastic scattering of final hadrons or the intermediate Δ^{++} on intranuclear neutrons not resulting in the change of the reaction topology; *d)* and *e)* background reactions followed, respectively, by a charge-exchange secondary interaction or by a pion absorption on a nucleon pair resulting in the change of the reaction topology, so that the latter imitates that of the reaction (1).

The shapes of the p_L^{miss} - and p_T^{miss} - distributions corresponding to the processes *a)*-*e)* are determined by Monte-Carlo simulations and presented in Figure 1. The normalization of the depicted curves will be discussed below. The simulated processes are:

a) The reaction on hydrogen

The simulation code includes several sources of the experimental uncertainties: the error in the three-momentum measurement for final particles, the minor effects related to the neutrino beam divergence and the muon inner bremsstrahlung (see [12] and references therein), as well as to the particle misidentification in a fraction of events with two non-identified positive hadrons (see Section 2 above). The simulated distributions $f_a(x)$ (x being p_L^{miss} or p_T^{miss}), shown in Figure 1 by dot-dashed curves, describe the sharp peak near $p_L^{miss} \sim 0$, as well as an essential fraction of the p_T^{miss} - distribution at very low values of $p_T^{miss} < 0.05$ GeV/c corresponding to the reaction (1) on the hydrogen.

b) The Fermi-motion of the bound proton

In addition to the effects described in item *a)* above, the Fermi-motion of the target proton is introduced (according to [13]) leading to a further widening of the distributions on p_L^{miss} and p_T^{miss} . The simulated distributions $f_b(x)$, as it is seen from Figure 1 (the dashed curves),

are responsible for a prominent fraction of events with low $|p_L^{miss}|$ and p_T^{miss} .

c) The intranuclear scattering of neutrino-produced hadrons

In addition to the effects described in items *a)* and *b)* above, we included in the simulation code the elastic scattering of neutrino-produced hadrons on intranuclear neutrons, provided that the proton and π^+ escaped any other interactions which could lead to the changing of the reaction topology. The elastic differential pn and π^+n cross sections and inelastic proton-nucleon and pion-nucleon cross sections are taken from compilations [14, 15, 16, 17]. A characteristic feature of the simulated distributions $f_c(x)$, the shapes of which are depicted by dotted curves, is their spreading over a wide range of p_L^{miss} and p_T^{miss} and, for the case of p_L^{miss} , a shifting toward positive values (also observed experimentally). The reason for this shifting is that in an elastic scattering the hadron energy E^i decreases on an average in a lesser degree than its longitudinal momentum p_L^i (cf. Eq. 3). The said effects are also inherent for the elastic process $\Delta^{++}n \rightarrow \Delta^{++}n$. The shapes of the distributions $f_c(x)$ for the latter, inferred from simulations (using the relevant cross sections predicted theoretically in [3,18,19]), differ only slightly from $f_c(x)$. This difference will be taken into account when describing the experimental distributions plotted in Figure 1.

d) The background reactions caused by charge-exchange intranuclear interactions

In addition to the effects described in items *a)* and *b)*, we included in the simulation code several background processes which could imitate the topology of the reaction (1), namely: the reaction $\nu n \rightarrow \mu^- n \pi^+$ followed by the neutron elastic scattering, resulting in a recoil proton in the final state, and the reaction $\nu p \rightarrow \mu^- p \pi^0$ followed by the π^0 charge-exchange reaction $\pi^0 p \rightarrow \pi^+ n$. The shapes of the simulated distributions $f_{d'}(x)$ and $f_{d''}(x)$ for these reactions turned out to be very close to $f_c(x)$, hence, only the summary contribution from *c)* and *d)* can be considered when describing distributions plotted in Figure 1. We also estimated the possible contribution from the reaction $\nu n \rightarrow \mu^- p$ followed by an inelastic reaction $pp \rightarrow pn \pi^+$ and found it to be negligible (about 1%) in the subsample of events-candidates to the reaction (1).

e) The background reactions caused by a pion absorption on a nucleon pair

We included in the simulation code the reactions $\nu p \rightarrow \mu^- p \pi^+ \pi^0$ and $\nu p \rightarrow \mu^- n \pi^+ \pi^+ \pi^0$ followed by π^0 absorption on a neutron pair, $\pi^0(nn) \rightarrow nn$, as well as the reactions $\nu n \rightarrow \mu^- p \pi^+ \pi^-$ and $\nu n \rightarrow \mu^- n \pi^+ \pi^+ \pi^-$ followed by π^- absorption on a quasideuteron, $\pi^-(pn) \rightarrow nn$ (the details concerning the pion absorption probabilities can be found in [24,25] and references therein). Contrary to the processes *c)* and *d)*, the nuclear absorption of a neutrino-produced pion leads to a shifting of the p_L^{miss} -distribution towards negative values, because of the omission in (3) of a positive term $(E^\pi - p_L^\pi)$ corresponding to the absorbed pion. The simulated shapes $f_e(x)$ of the processes *e)* are depicted in Figure 1 by thin curves. We fitted together the p_L^{miss} - and p_T^{miss} -distributions with four-parameter expressions

$$F(x) = N_a \cdot f_a(x) + N_b \cdot f_b(x) + N_{cd} \cdot f_{cd}(x) + N_e \cdot f_e(x), \quad (5)$$

where x denotes p_L^{miss} or p_T^{miss} . All functions in (5) are normalized to unity. The function $f_{cd}(x)$ is a linear contribution of simulated distributions $f_c(x)$, $f_{c'}(x)$, $f_{d'}(x)$, $f_{d''}(x)$ with relative weights which were varied in wide ranges, in view of the lack of information on the expected contributions of subprocesses described in items *c)* and *d)*. The fit parameters N_a , N_b and N_e correspond to the event numbers of processes *a)*, *b)* and *e)*, while $N_{cd} = N_c + N_d$ is the summary number of events corresponding to the processes *c)* and *d)*. The fitted values of these parameters are equal to $N_a = 100 \pm 12 \pm 3$, $N_b = 246 \pm 36 \pm 9$, $N_{cd} = 148 \pm 25 \pm 13$ and $N_e = 66 \pm 39 \pm 21$, where the first error is statistical and the second one reflects the uncertainty in the relative weights of the subprocesses described in items *c)* and *d)*.

An example of the fit results is presented in Figure 1. Although the fit quality is not bad ($\chi^2/ndf \approx 1.8$), the fitted p_T^{miss} -distribution somewhat underestimates the data at relatively high values of $p_T^{miss} = 0.4 - 0.75$ GeV/c. This discrepancy can be, at least partly, caused by the fact that our simulation code uncorporate no more than one intranuclear scattering of a given hadron.

The inferred value of N_a is in good agreement with the expected value of $N_p^{free} = 115 \pm 21$ (cf. Section 2), thus indicating the self-consistency of our results. The value of N_b , corresponding to the number of events on bound protons (possessing Fermi-motion) not followed by any secondary interaction, composes $60 \pm 13\%$ of the expected total number $N_p^{bound} = 411 \pm 65$ of events occurred initially via the channel (1) on bound protons (cf. Section 2). Hence, the probability of secondary intranuclear interactions, both violating or not the topology of the reaction (1) is equal to $P_{int} = 0.40 \pm 0.13$. Further, we estimated from simulations that the probability P_c of the process c) with respect to the probability P_{int} composes $P_c/P_{int} = 0.36$, resulting in $P_c = 0.14 \pm 0.05$ and hence the event numbers $N_c = P_c \cdot N_p^{bound} = 59 \pm 27$ and $N_d = 89 \pm 38$.

The number N_c along with N_b gives the number of survived events of the reaction (1) on bound protons, $N_b + N_c = 305 \pm 33$ composing $74 \pm 8\%$ of N_p^{bound} , while the remaining $26 \pm 8\%$ of events turn out to be rejected due to secondary interactions violating the reaction topology.

It should be also noted, that the total number of survived events of the exclusive reaction (1) both occurred on free and bound protons is equal to $N_{exc} = N_a + N_b + N_c = 405 \pm 36$, with a rather small fraction of $N_c = 59 \pm 27$ events in which the neutrino-produced proton and/or π^+ meson suffered an elastic scattering on intranuclear neutrons. We conclude, therefore, that in the case of the $\Delta^{++}(1232)$ production in the exclusive channel (2) the deterioration of its spectral function due to these elastic interactions is expected to be faint.

4. THE $\Delta^{++}(1232)$ EXCLUSIVE PRODUCTION

For the analysis of the π^+p effective mass distribution, the events with $|p_L^{miss}| < 0.4$ GeV/c and $|p_T^{miss}| < 1$ GeV/c were selected. This allow us, as it follows from Figure 1, to save practically all events of the reaction (1) and to reject a fraction of events belonging to the background reactions described in the items d) and e) of the previous section. The π^+p effective mass distribution is plotted in Figure 2. Apart from a clear Δ^{++} signal, a comparatively narrow peak is seen around 1.6 GeV/c² which can correspond to the narrowest excited state of Δ^{++} , namely, the S_{31} -wave $\Delta^{++}(1620)$ with the Breit-Wigner mass ~ 1630 MeV/c² and the full width $\Gamma \approx 145$ MeV (see [22]). Other Δ^{++} states with masses up to 2 GeV/c² are too wide ($\Gamma \sim 200 \div 500$ MeV) and hence cannot be disentangled from the non-resonance background. Moreover, their signals are expected to be practically invisible due to their small π^+p decay fraction [22].

To describe the mass distribution we used a fit function

$$N(m) = N(1232) \cdot [(1 - P_c) \cdot BW_{1232}^{exp}(m) + P_c \cdot BW_{1232}^{scat}(m)] + N(1620) \cdot BW_{1620}^{exp}(m) + BG(m), \quad (6)$$

being the sum of two simulated Breit-Wigner functions [23] for $\Delta(1232)$ and $\Delta(1620)$, smeared according to the experimental inaccuracies, and a smooth background function assuming that it involves the contributions both from the non-resonant background inherent to the reaction (1) and from the background processes described in the items d) and e)

above, as well as the summary contribution from all large-width ($\Gamma > 150$ MeV) Δ^{++} states. The background function was parametrized by a simplest form $BG(m) = \alpha m^\beta \exp(-\gamma m)$. Besides, we included in the fit function the simulated distribution $BW_{1232}^{scat}(m)$ corresponding to the elastic scattering of the $\Delta^{++}(1232)$ decay products on intranuclear neutrons. The probability of the latter $P_c = 0.14 \pm 0.05$ was estimated in the previous section. In this case, a factor $1 - P_c$ was introduced for the $\Delta(1232)$ spectral function $BW_{1232}^{exp}(m)$ which did not incorporate scattering effects. Due to the smallness of the $\Delta(1620)$ contribution to the π^+p mass distribution and of the scattering probability P_c , we neglected the scattering effects in its spectral function $BW_{1232}^{exp}(m)$. Note, that all Breit-Wigner functions in (6) are normalized to unity.

An example of the fit result at $P_c = 0.14$ is plotted in Figure 2. The thin solid and dotted curves correspond to the $\Delta(1232)$ production followed or not by secondary scattering processes with probabilities, respectively, $P_c = 0.14$ and $1 - P_c = 0.86$. The dot-dashed and dashed curves correspond to the $\Delta(1620)$ production and the background distribution. The sum of these four contributions is depicted by the thick solid curve which satisfactorily describes the experimental data (with $\chi^2/ndf = 1.2$). It should be noted, that the limited statistics of our data does not allow to infer any conclusion concerning the mass shift and the widening of the $\Delta^{++}(1232)$ resonance caused by its propagation in the nuclear medium [2, 3, 4].

The fit results in the numbers $N(1232)$ of produced $\Delta^{++}(1232)$, (both followed or not by secondary elastic scattering of the decay products) and $N(1620)$ of $\Delta^{++}(1620)$ (for the decay mode of π^+p) being equal to $N(1232) = 230 \pm 30 \pm 8$ and $N(1620) = 40 \pm 25 \pm 1$, where the quoted errors reflect, respectively, the statistical uncertainty and the uncertainty in $P_c = 0.14 \pm 0.05$. The corresponding mean yields, normalized to the event number $N_{exc} = 405 \pm 36$ of the exclusive reaction (1), are equal to $\bar{n}(1232) = 0.57 \pm 0.09$ and $\bar{n}^{corr}(1620) = 0.40 \pm 0.25$, the latter being corrected for the π^+p decay fraction ($25 \pm 5\%$) [22].

It should be noted that the mean yield of $\Delta^{++}(1232)$ underestimates the cross section ratio $r_{exp} = \sigma(\nu p \rightarrow \mu^- \Delta^{++})/\sigma(\nu p \rightarrow \mu^- p \pi^+)$ deduced from available experimental data on free protons, $r_{exp} = 0.85 \pm 0.14$ at $\langle E_\nu \rangle = 3$ GeV [24] and $r_{exp} = 0.79 \pm 0.16$ at $\langle E_\nu \rangle = 27$ GeV [25], as well as from theoretical calculations at $\langle E_\nu \rangle \sim 9$ GeV: $r_{theor} \approx 0.92$ (see [10, 25] and references therein). We conclude, therefore, that the nuclear absorption effects are more prominent in the channel (2) as compared to the channel (1). This 'extra' absorption can be quantified by a factor $r_{theor}/\bar{n}(1232) = 1.61 \pm 0.25$. The observed suppression of the $\Delta^{++}(1232)$ yield can be, at least partly, explained by its large absorption cross section via the channel $\Delta^{++}n \rightarrow pp$ on intranuclear neutrons [2, 3, 26].

5. SUMMARY

For the first time, the nuclear effects influencing the kinematic characteristics of the reaction $\nu p \rightarrow \mu^- p \pi^+$ (1) on bound protons are studied and explained by the Fermi-motion of the target proton and secondary elastic scattering of neutrino-produced hadrons on intranuclear neutrons. The probability of any intranuclear interaction of neutrino-produced hadrons is extracted: $P_{int} = 0.40 \pm 0.13$, while the probability of interactions occurring only via elastic scattering on intranuclear neutrons is estimated to be $P_c = 0.14 \pm 0.05$.

A clear evidence of the $\Delta^{++}(1232)$ and an indication on the $\Delta^{++}(1620)$ isobar states production in the reaction (1) are observed, with the mean yields $\bar{n}(1232) = 0.57 \pm 0.09$ and $\bar{n}(1620) = 0.40 \pm 0.26$ (the latter being corrected for the $\Delta^{++}(1620) \rightarrow p \pi^+$ decay fraction).

The mean yield of $\Delta^{++}(1232)$ is by 1.61 ± 0.25 times smaller than expected for the reaction (1) on the free proton, thus indicating on its noticeably nuclear absorption before its decay.

ACKNOWLEDGMENTS

The authors from YerPhI acknowledge the supporting grants of Calouste Gulbenkian Foundation and Swiss Fonds Kidagan. The activity of one of the authors (H.G.) is supported by Cooperation Agreement between DESY and YerPhI signed on December 6, 2002.

References

- [1] N.M.Agababyan *et al.*, YerPhI Preprint No. 1619(3), (2008); arXiv:0811.2343
- [2] S.Boffi *et al.*, Yad. Fiz. **60**, 1320 (1997)
- [3] L.A.Kondratyuk, Yu.S.Golubeva, Yad. Fiz. **61**, 951 (1998)
- [4] H.Kim, S.Schramm and S.H.Lee, Phys. Rev. C **56**, 1582 (1997)
- [5] V.V.Ammosov *et al.*, Fiz. Elem. Chastits At. Yadra **23**, 648 (1992)
- [6] N.M.Agababyan *et al.*, Preprint No. 1535, YerPhI (Yerevan, 1999)
- [7] N.M.Agababyan *et al.*, Yad. Fiz. **66**, 1350 (2003)
- [8] S.I.Alekhin *et al.*, Compilation of cross sections IV, CERN-HERA, 87-01 (1987)
- [9] J.Brunner *et al.*, Z. Phys. C **42**, 361 (1989)
- [10] H.J.Grabosh *et al.*, Z. Phys. C **41**, 527 (1989)
- [11] D.Allasia *et al.*, Nucl. Phys. B **343**, 285 (1990)
- [12] H.C.Ballagh *et al.*, Phys. Rev. Lett. **50**, 1963 (1983)
- [13] Y.Haneshi and T.Fujita, Phys. Rev. **33**, 260 (1986)
- [14] O.Benary, R.Price and G.Alexander, UCRL-20000 NN, 1970
- [15] V.Flaminiio *et al.*, CERN-HERA 79-03, 1979
- [16] E.Bracci *et al.*, CERN-HERA 75-2, 1975
- [17] V.Flaminiio *et al.*, CERN-HERA 83-01, 1983
- [18] G.Mao, Z.Li and Y.Zhuo, Phys. Rev. C **53**, 2933 (1996)
- [19] T.-S.H.Lee, Phys. Rev. C **54**, 1350 (1996)
- [20] V.M.Asaturyan, A.G.Khudaverdyan and H.R.Gulkanyan, Nucl.Phys. A **496**, 770 (1989)
- [21] N.M.Agababyan *et al.*, Z. Phys. C **56**, 371 (1992)
- [22] C.Amsler *et al.*, Phys. Lett. B **667**, 1 (2008)
- [23] J.D.Jackson, Nuovo Cim. **34**, 1664 (1964)
- [24] W.Lече *et al.*, Phys. Lett. **78** B, 510 (1978)
- [25] J.Bell *et al.*, Phys. Rev. Lett. **41**, 1008 (1978); *ibid.* **41**, 1012 (1978)
- [26] G.Mao *et al.*, Phys. Rev. C **57**, 1938 (1998)

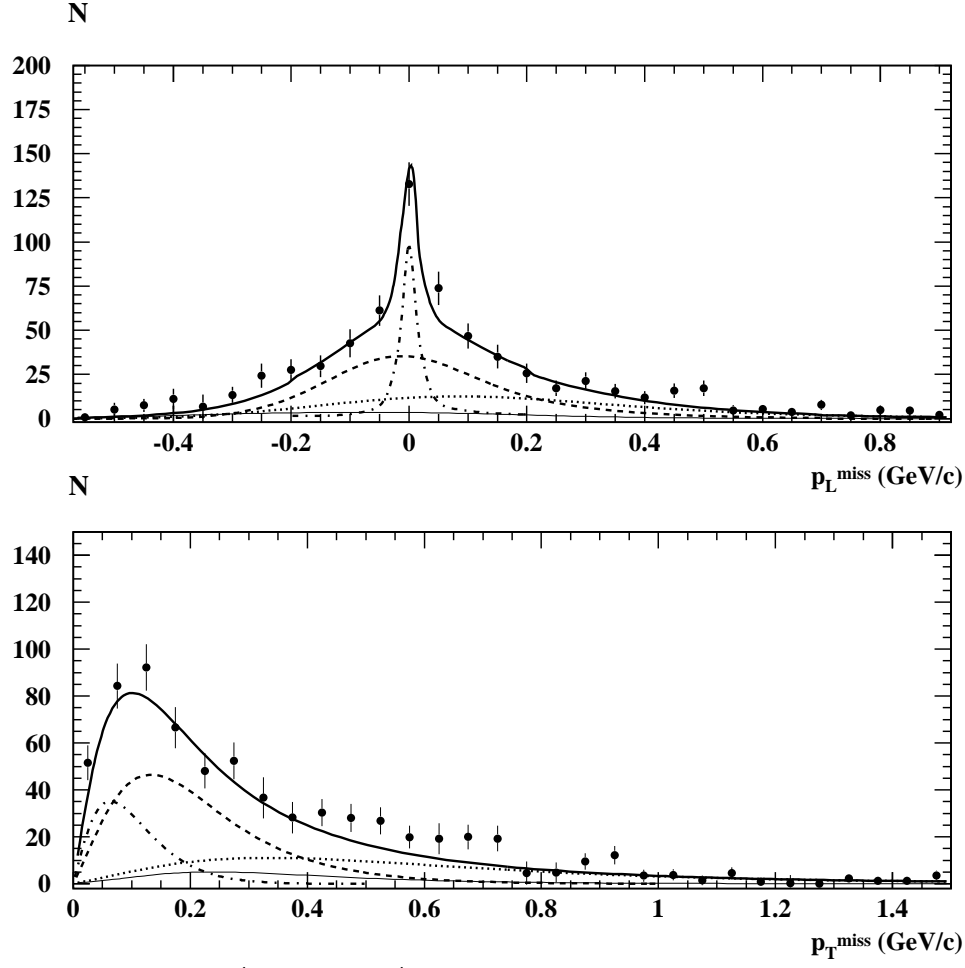


Figure 1: The p_L^{miss} - and p_T^{miss} - distributions. The curves are the fit results (see the text).

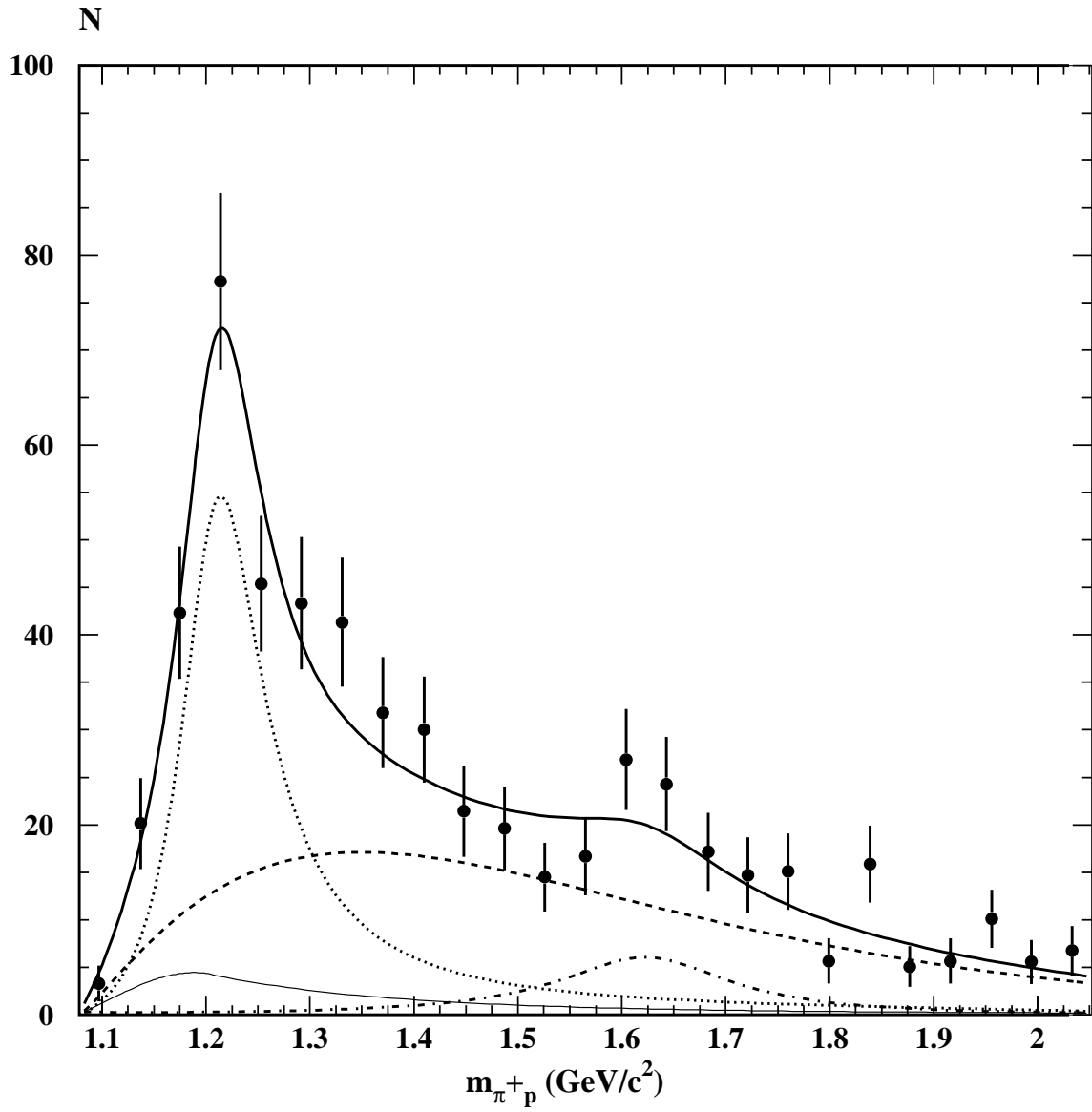


Figure 2: The π^+p effective mass distribution. The curves are the fit results (see the text).